Louisiana Sea Grant Undergraduate Research Opportunity Program (UROP)

Final Report

Evaluation of a Microfluidic Device to Standardize Sperm Motility Assessment in Louisiana Saltwater Fishes

Undergraduate Student Researcher: Val Browning

Department of Biological and Agricultural Engineering

Louisiana State University, Baton Rouge, LA, USA

January 31, 2021

Faculty Advisor: W. Todd Monroe, PhD

Project Co-advisor: Yue Liu, PhD

Abstract

Standardized assessment of sperm quality is important for (1) development of sperm repository by cryopreservation for fish stock enhancement, and (2) evaluation of the impact of environmental pollution to animals using bioindicator species. Variation of user techniques and outcomes exists across laboratories performing sperm activation, accomplished by mixing sperm and seawater manually. Microfluidics technology has shown potential to address this problem by providing standardized sperm mixing and activation that enable sperm motility being assessed using existing microscopic analysis methods. In this project, a novel microfluidic chip was developed for standardized analysis of sperm quality of Louisiana saltwater fish species. COMSOL Multiphysics and Autodesk Inventor were used for design and simulation. Two candidate designs were chosen after an iterative design/simulation process. Photomasks for the fluidic layer of both candidate designs were manufactured. The template mold for the primary design was fabricated using manual mask alignment. The device was fabricated by molding a curable elastomer on the template. The device was tested for flow initiation/cessation, ease of loading and operation, and preliminary testing was done for evaluating mixing efficiency.

1. Introduction

Standardized evaluation of sperm motility is important for development of sperm repositories by cryopreservation for stock enhancement programs for recreational fishes. For example, the red snapper (*Lutjanus campechanus*) is economically important for recreational and commercial fisheries. Red snapper wild stocks in the Gulf of Mexico experience pressures from fishing, habitat degradation, and capture as bycatch in trawl fisheries (Chesney *et al.* 2000). Fishery managers have made efforts to protect and enhance wild stocks of red snapper, including harvest quotas (Goodyear 1995), and development of hatcheries (Riley *et al.* 2004; Williams *et al.* 2004). Cryopreservation protocols for red snappers were developed to preserve the genetic diversity of broodstock through sperm repositories. Sperm motility assessment is also useful for evaluation of impact of environmental pollution to animals using aquatic species as bioindicators. Sperm motility of Eastern Oysters (*Crassostrea virginica*) were used to evaluate environmental impacts of the Deepwater Horizon disaster.

Although sperm motility is the most important and widely used parameter to assess sperm quality (Fauvel *et al.* 2010), techniques to evaluate sperm motility is problematic because of a lack of standardization. Highly variable procedures of motility evaluation across different laboratories make it difficult or impossible to directly compare research results (Liu *et al.* 2019). Specifically, to evaluate motility, fish sperm must be activated via exposure to a hypotonic environment for freshwater species and hypertonic media for saltwater species, and once activated the peak motility is limited by a short period (5-20 sec) (Alavi and Cosson 2006). As such, the time window of mixing sperm with activation solution and loading sample onto to a slide (or chamber) to be

evaluated using microscopy is critical, because a difference of seconds could affect motility results (Beckham *et al.* 2018). However, the procedures and techniques are highly variable among laboratories and researchers, resulting in low reproducibility of research related to fish sperm motility (Hagedorn *et al.* 2019).

In this report, the creation of a microfluidic device capable of passively mixing small volumes of fluid will be described. Microfluidic technology, also called "lab-on-a-chip" technology, utilizes microfabrication methods to develop devices capable of confining large-scale laboratory practices to micrometer scales (Whitesides 2006). Microfluidic chips can easily handle small-volume (<μL) samples within automated analysis tools, offering advantages such as low sample consumption, low cost, high portability, and high standardization. This emerging technology has been widely used in human fertility research and sperm-related disease diagnosis with commercial products approved by the USDA (Kashaninejad *et al.* 2018). However, the potential of microfluidic chips to assist sperm analysis has not been well recognized in the field of aquaculture and fisheries.

To our knowledge, no microfluidic devices or relevant studies have been reported for sperm motility analysis of saltwater fishes. Such microfluidic devices can provide functions of 1) flow control by a micro-pipette adaptor, 2) sample mixing by unique geometries to mix sperm and diluent, and 3) ensuring rapid analysis of the sperm motility after mixing through a microscope at a viewing region on the microfluidic channel using of computer-assisted sperm analysis (CASA) system. Our prior work (Beckham *et al.* 2018) has shown the feasibility of using microfluidic devices to evaluate sperm motility on a freshwater fish (zebrafish *Danio rerio*), however, thisdevice was problematic because of the difficulty in sample introduction, low mixing ratio (1:2 which did not provide sufficient mixing for sperm activation), and flow control (due to a narrow channel width). Thus, this project aimed to develop and evaluate a microfluidic device with novel functionalities, including easy flow initiation with common laboratory pipettes, high mixing ratio to ensure sperm activation, and minimal pressure drop to enable rapid flow cessation.

The goal of this research project was to evaluate the functionality of a microfluidic device to assist standardization of sperm activation and motility analysis from saltwater fish species in Louisiana. Starting with a preliminary device design, which was conceptualized in a capstone course at LSU, the device was redesigned using various finite-element-analysis (FEA) simulation and computer-aided design (CAD) software. The specific objectives of this project were to: 1) Evaluate mixing efficiency and pressure drop across microchannels in the device and enhance the mixing efficiency from the preliminary design, 2) Fabricate the device with a soft lithography process, assemble and load the device, and evaluate these prototypes with artificial microbeads and particle image velocimetry (PIV) techniques; and 3) Evaluate functionality of the device, including mixing efficiency, flow cessation, and sperm activation efficiency.

2. Materials and Methods

2.1 Improvement of channel geometry through simulation analysis

2.1.1 Previous work and motivation

Preliminary designs for the microfluidic device were created by a group of students, including Val, who were enrolled in LSU's Biological Engineering capstone project course. The initial device design was fabricated and tested in a laboratory setting (Fig. 1). The device's fabrication process involved the creation of two photomasks, which were used with photolithography to produce template molds on a silicon wafer (Fig. 2). Disposable devices were cast on these molds from polydimethylsiloxane (Sylgard-184) and a curing agent, then irreversibly bonded to glass microscope slides by plasma-oxygen treatment. Device operation consisted of wetting the device, loading the inlet ports with fluids, and connecting the outlet port to a negative pressure source while viewing the large, main microchannel under a microscope.

Observations made during the fabrication and testing process such as difficult photomask alignment (Fig.2), imbalanced flow from inlet microchannels (Fig. 3), and microchannel clogging necessitated a device redesign. Simulation results from COMSOL Multiphysics showed that pressure drops (from the leftmost edge of the figure to the edge of each inlet port) were not equal, likely due to a difference in channel length between the central, looping channel and the arched channel pairs. The addition of the tapered region on the shorter arched channels contributed to clogging with fibrous material or debris and occasionally rendered devices unusable after testing or cleaning.

The newly proposed designs address these issues from the perspective of easing device usability and handling, with the geometries being altered specifically to achieve a desirable sample mixing ratio (6:1) and equalize pressure differentials across all microchannels.

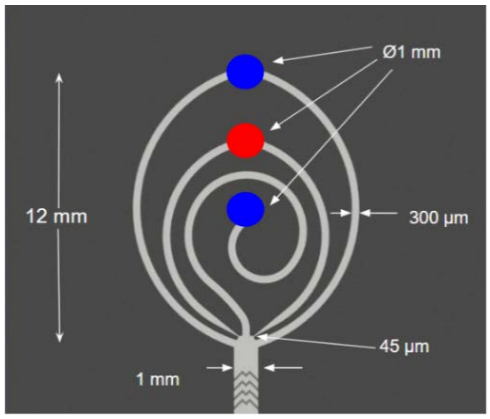

Fig. 1: Preliminary device design, shown zoomed to the microfluidic inlets for water/buffer solution (blue) and sperm sample (red). The novel micromixing geometry is shown at the bottom of the image, and consists of a unique 'herringbone' microstructure array designed to mix the laminar flow pattern.

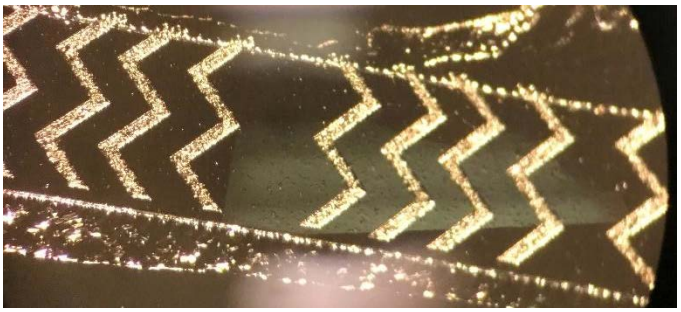

Fig. 2: Best result from mold fabrication of previous design using manual photomask alignment. The lower edge of the microchannel shows clear misalignment of the mixing geometry, which was thought to lead to less efficient mixing due to misalignment of the structure peaks with the sperm sample streams.

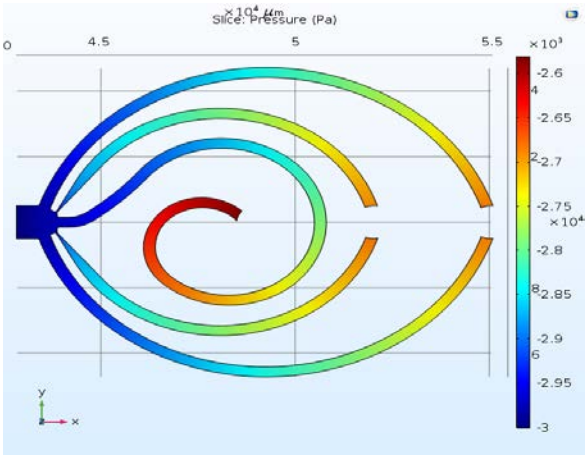

Fig. 3: COMSOL Multiphysics simulation results for a subsection of the microfluidic layer of the device.

2.1.2 Design / simulation process

COMSOL Multiphysics was used for finite element analysis simulations that aided in the design process, focusing on generating equal pressure drops across parallel microchannels and desirable chemical species transport by induced mixing of laminar flow. The former is necessary for the device to properly function, as this constraint ensures equal bulk fluid flow from each inlet. To ease the simulation process and to avoid simulating the entire device, modifications to the full geometry were made to simplify simulations. Specifically, the inlet port geometry was removed from the end of each microchannel and replaced with a positive constant pressure boundary condition, to represent the static fluid head of the loaded ports.

Each candidate design was first simulated without the mixing structures and complete main channel, as it was imperative to determine the location of the center point of each sample stream as measured laterally across the channel, so that the peaks of the chevron mixing structures could be properly aligned. Simulating the entire length of the channel was not

necessary, as previous results showed little variation in streamline width or species transport downstream of the junction. The procedure used with both Autodesk Inventor and COMSOL to simulate fluid flow and species transport was similar for each design. First, a sketch of the microchannels would be made in Inventor and extruded 25 um, as this is the intended channel height. The mixing structures, when included, were extruded an additional 25 um as a two-step photolithography process was used to create the mold. Next, the Inventor CAD model was linked to COMSOL using LiveLink, an add-on that creates an interface between the programs and facilitates the importation of complex geometries. This allowed easy modification of the simulated geometries, as well parametric modeling of features such as micromixer position and channel dimensions.

Within COMSOL, a standardized study setup was used for each design iteration. The process involved creating a mesh for the geometry, defining the material and simulation boundary conditions, and running the solver. Meshing was a nontrivial part of the simulation process, and resources such as COMSOL example projects and forums provided necessary information for the creation of an optimal mesh for these studies. The mesh was designed as a swept mesh from the top XY face of the part to the bottom. This allowed control of the number of layers in the Z- direction, which was minimized as variation of fluid parameters in the Z direction was expected to be negligible, except for wall effects. Mesh size parameters were manually adjusted to achieve a maximum element size of no more than 20 um^2 for each mesh.

Simulations of the original design showed a lower mixing ratio than anticipated (Fig. 4). The channels with streamlines were intended to taper the width of the sample fluid stream to increase the device's mixing ratio. Instead, the streams take up a larger width than expected, which was undesirable as a design goal was to achieve a higher mixing ratio. The flaws of the original device led to experimental trial inconsistency with devices fabricated and tested experimentally, and the proposed redesign in this report intends to improve upon these flaws, using COMSOL and Autodesk Inventor as the main design tools.

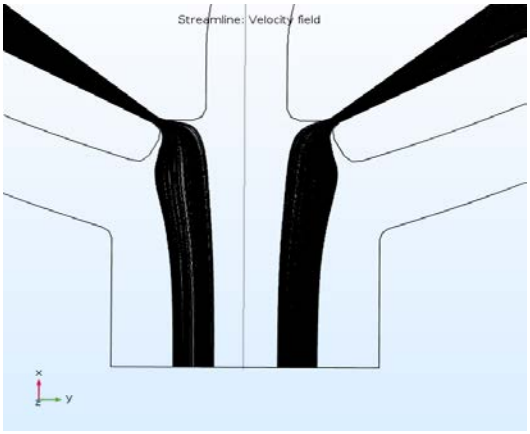

Fig. 4: Fluid streamlines from COMSOL simulation of previous device design.

2.1.3 Preliminary designs

The new device had multiple design iterations, using COMSOL as the guiding tool. First, the previous device's design was simplified so that an analytical method could be used to aid in the initial redesign. Poiseuille's Law was used as a starting point for redesigning the channels, as it relates pressure drop, flow rate, and channel geometry. To determine the lengths of each channel, the flow rates in Poiseuille's Law were constrained so that the desired mixing ratio would be preserved (Kirby 2013). Next, the pressure drops across each microchannel were set equal, which was another design constraint to ensure stable flow. Thus, the channel lengths were adjusted (changing the channel's hydrodynamic resistance) to roughly approximate a solution to Poiseuille's Law satisfying the design constraints. This step involved replacing the curved microchannels (Fig. 1) with linear channels such that each channel connects to a unique inlet port. This was understood to increase the complexity of the buffer/sample loading procedure, but only two additional pipetting actions are required in comparison to the original design. The lengths and widths of these linear channels were constrained by the desired mixing ratio and the requirement of equal pressure drops across each channel. In each design, the wider buffer channels had a width of 285.7 um, the narrower sample introduction channels had a width of 71.4 um, and the main channel downstream from the junction had a width of 1 mm. Given equal pressure drops across the channels, the diluent/sample ratio in the resultant laminar flow would equal the ratio of the widths of the respective introduction channels (Kirby 2013).

The first design can be seen in Fig. 5 and consists of linear microchannels that approach the fluid junction. This channel arrangement was chosen as a starting point for geometry improvement, as previous experiments with a device consisting of a simple T-junction were successful. However, simulations of flow patterns in this device were shown to produce large areas of lower static pressure where the horizontal channels overhang the main channel, which caused the sample fluid streamlines to bulge and become wider than the channels which carried the fluid to the junction. This was undesirable as tight control over both the location and width of the sample fluid streams would assist in increasing mixing efficiency, by ensuring that the fluid was evenly distributed by the mixing geometry and the mixing ratio between sample and diluent was maximized.

In the next design iteration, the buffer/sample introduction channels were rotated such that the angle between each of them was decreased, and the angle between the outer diluent channels and the main channel was increased. COMSOL simulation results for both sample fluid streamlines and dilute species transport showed a more desirable flow pattern that emerged when the inlet channels were more closely aligned with the main channel.

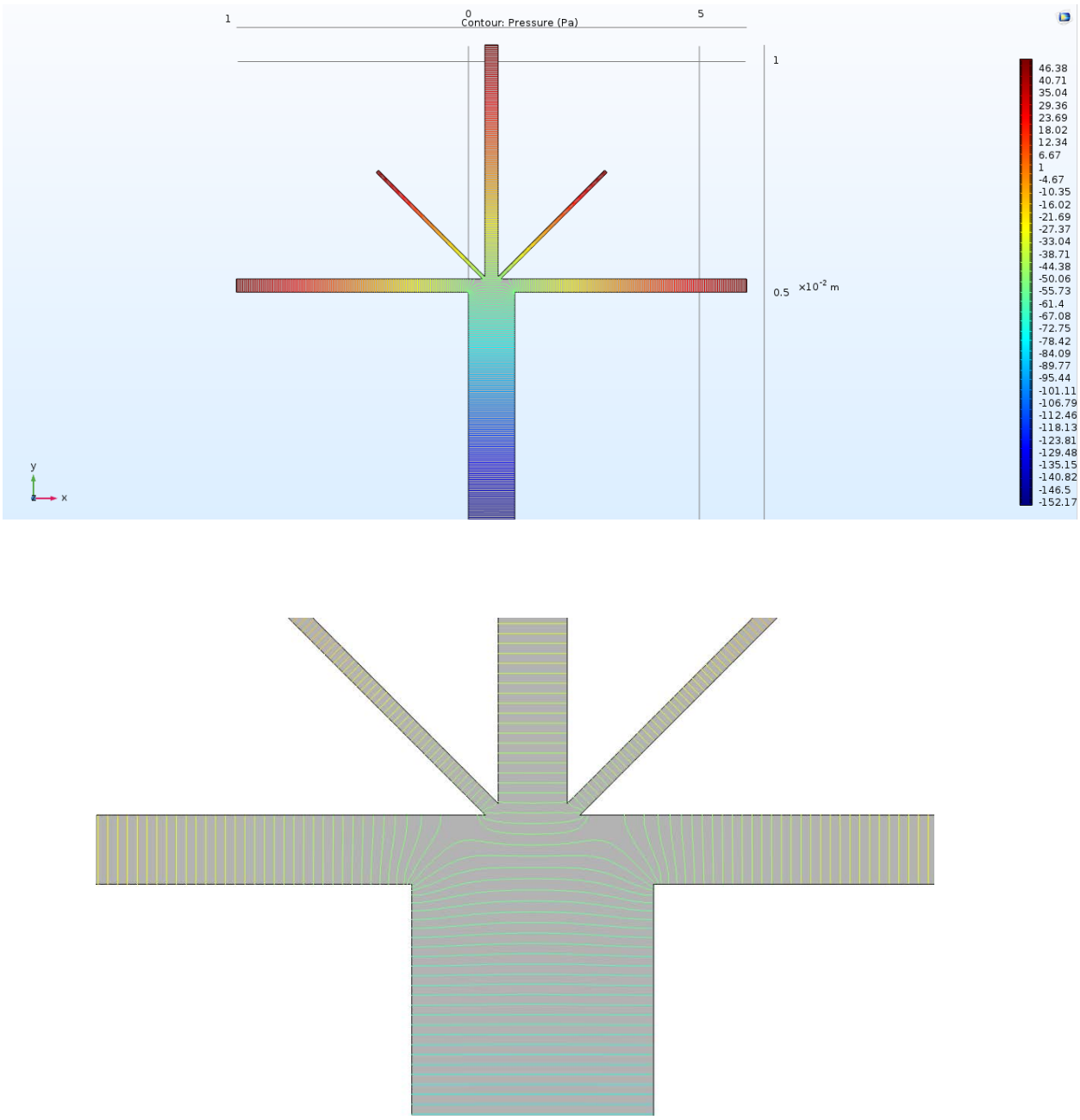

Fig5. First design iteration (upper), showing linear channels at 0, 45, 90, and 135 degrees from normal in the XY plane. Color results show equal-pressure contours. A zoomed image (bottom) of the contours at the fluidic junction.

2.1.4 Final candidate designs

Several candidate designs were developed, and two were chosen to send to CAD/ART for photomask printing. The designs were both improvements over the standard T-junction channel and consisted of straight channels of constant width that joined at a common junction. Both

designs were similar, but offer different potential advantages and disadvantages with regard to fabrication and operation. The primary candidate design (Fig. 6) was achieved by decreasing the angle between the fluid introduction channels and increasing the angle between the outermost channels and the main channel. COMSOL results (Fig. 7) showed that the resulting laminar flow pattern was more predictable and introduced less lateral diffusion than the basic T-junction design. The secondary candidate design (Fig. 8) applied the same changes to the T-junction design but keeps the channels slightly wider to increase the minimum angle needed to be patterned. Previous observations with thin channel geometries and extremely acute angles in the fabrication process presented potential challenges for the primary design. In particular, the sample introduction channels, and the middle diluent channel form a small angle, which was thought to be either difficult to properly expose with UV given our current equipment, or be a point of structural weakness with repeated device use. As such, the secondary design alleviates this issue by having a larger minimum feature angle but may introduce more lateral diffusion and less-desirable pressure contours at the junction (Fig. 8).

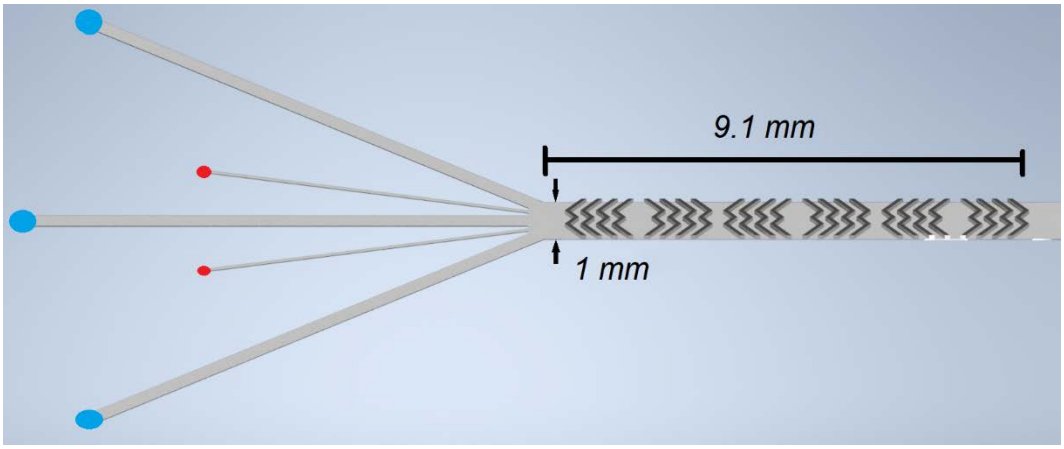

Fig. 6: Primary candidate design for microfluidic device, showing inlet ports for water/buffer solution in blue and for sperm sample in red. The complete micromixer geometry is shown, and the viewing region for CASA lies to the right of the structures.

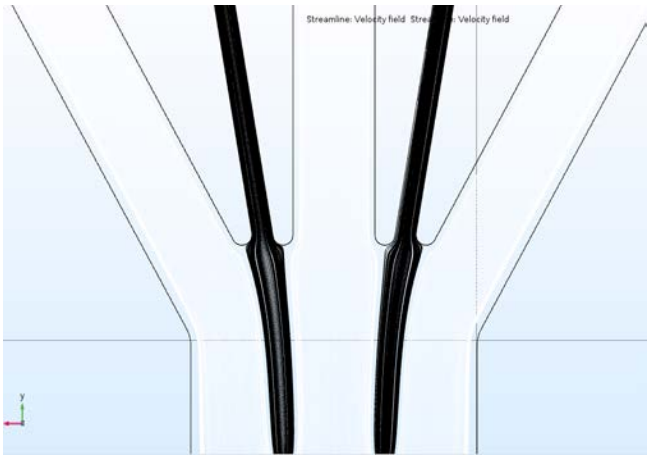

Fig. 7: COMSOL streamline results for primary candidate design, showing streams of relatively equal widths upstream and downstream of the junction

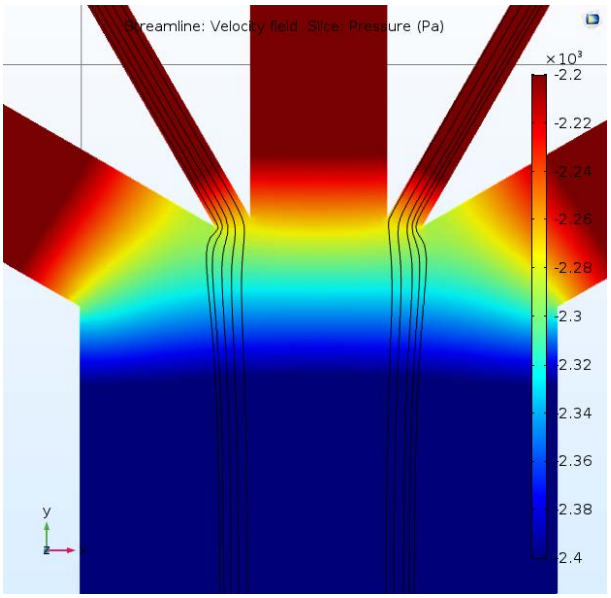

Fig. 8: COMSOL composite results for secondary candidate design, showing pressure contours around the junction and streamlines from the sample introduction channels.

2.2 Device fabrication process

2.2.1 Photomask design

Template mold fabrication required the purchase of four photomasks, each with a unique pattern designed to be used in the photolithography process. Two masks were designed for the fluidic layers of two candidate designs, and two masks were designed with micromixing geometry. Of the two photomasks outlining the mixing geometry, one was designed with the width of the mixing structures equal to the width of the main channel (1 mm) and one was

designed with a slightly larger width of mixing structures, to allow for slight photomask misalignment. The photolithography process has been previously attempted with photomasks created in-house with various techniques, but these were inferior to masks ordered from an outside printing source. For this project, CAD/ART services (outputcity.com, based in Bandon, Oregon) was the distributor for photomask printing.

2.2.2 Multi-step photolithography

A template mold of the device was created using a multi-step photolithography protocol. This process involves precisely depositing a layer photoresist (SU-8 2025) onto a silicon substrate, exposing the substrate to ultraviolet light through a photomask, and various baking/cleaning steps, followed by a final development and bake. This method requires multiple rounds of spin-coating the photoresist and exposing the substrate since the design requires features to be fabricated at different heights. Specifically, the fluidic layer (Fig. 9) was fabricated at a height of 25 um, and the mixing structures (Fig. 9) were made on top of the previous step at a height of 25 um, for a total height of 50 um in regions which were UV-exposed twice.

Proper alignment of the photomasks for multi-step photolithography is handled most precisely by contact mask aligners, but manual mask alignment can be feasible with practice and experience. Techniques used by Benesch-Lee *et. al* were used to assist with manual photomask alignment as an optical mask aligner was not available. Specifically, the silicon substrate was fixed on a piece of stock PMMA plastic using tape, and manual alignment tracing was done in attempt to restrict the substrate's movement during mask alignment. After the first mask was used for UV-exposure, the substrate was again fixed to the stock plastic while the second mask was aligned, using tracing marks and the substrate's perimeter as a guide. Due to the small feature size, misalignment may not be detected until the development step, meaning that most of the mold fabrication process is wasted if alignment is not suitable for device fabrication. For the template mold made using the primary candidate design, there was a rotational misalignment that led to some mixing structures overlapping the channel edge (Fig. 10), but the features were within tolerance of a previous device which was operational despite misalignment. More precise methods for manual mask alignment, as well as use of a contact aligner, are currently being explored by the lab.

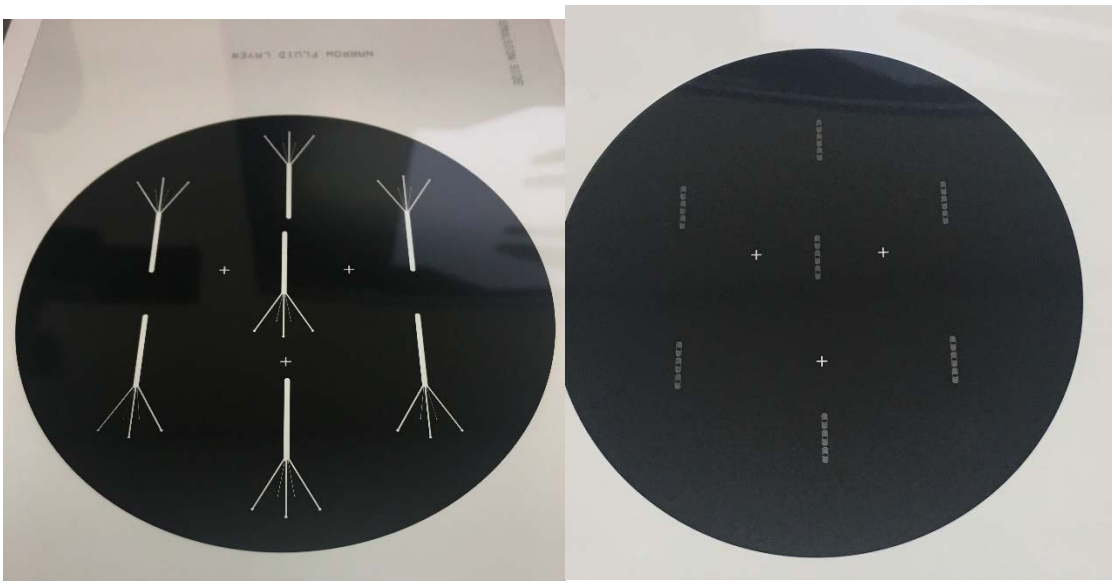

Fig. 9: Photomasks printed by CAD/ART. Masks are circular to match the 10.5 mm diameter silicon substrate. Fluidic layer (left), and herringbone micromixing geometry (right).

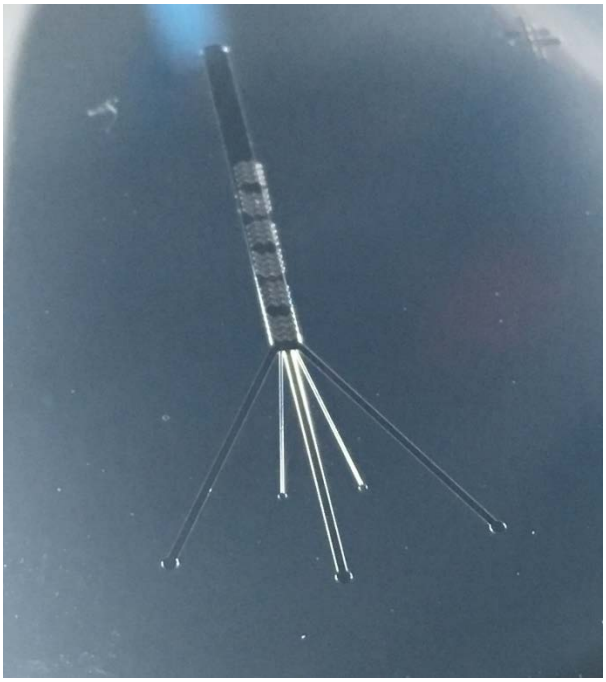

Fig. 10: Template mold of primary candidate design, consisting of features patterned in SU-8 photoresist cured and baked on a silicon substrate. Alignment marks can be seen in the upper-right corner.

3 Results and Discussion

3.1 Mold fabrication and device assembly

3.1.2 Device Fabrication

The device was designed to handle small volumes of sample/buffer solutions, as well as operate by inducing/stopping flow with a handheld micropipette. The device was fabricated by casting a silicone elastomer and curing agent mixture onto the template mold, and baking in a convection oven at 75°C. The elastomer used was polydimethylsiloxane, or Sylgard-184, a commonly-used material to produce microfluidic devices. For this device and many produced in this lab, a 10:1 ratio of elastomer and curing agent is measured and mixed before casting.

After demolding the cured elastomer and using a blade to cut individual patterned parts, a 1 mm biopsy punch was used to create user access ports for the microchannels. Punches were made at the end of each microchannel, while care was taken not to overlap a punch with the edge of another channel. After inspecting the elastomer for any hanging material and manually cleaning loose debris, the pieces are washed and air-dried, to avoid fibrous material from absorbent paper to attaching to the piece. Finally, the pieces were plasma treated for 30 seconds alongside glass microscope slides, which are then used to irreversibly seal the device.

3.2 Device functionality evaluation

Once the device was fabricated and sealed, testing could begin and would follow a similar regime to that conducted by the capstone engineering team with the previous design: testing of flow generation / cessation with a handheld pipette or syringe pump, evaluating mixing by testing the device with dye or fluorescein, loading the device with microbeads to simulate sperm cells for PIV analysis, and evaluating efficiency of sperm activation within the device.

3.2.1 Loading and operation with pipette/pump

To handle small volumes of sample fluid, the device’s access ports wereloaded manually by micropipette (Fig. 11). Specifically, 1 uL of sample was added to each of the two sample inlet ports, and 1 uL of diluent was added to the diluent ports. With 1 mm – diameter ports, it was difficult to avoid fluid cohesion and surface tension, which occasionally prevented fluid from settling in the port. As such, future devices will be fabricated with a larger-diameter biopsy punch, to allow the pipette tip to make contact with the bottom of the port upon injection to ensure fluid rests at the lowest level.

To operate the device, a stable flow was desired to effectively introduce the sperm sample to the mixing region for activation and carry it downstream for CASA/PIV viewing. Three methods had been previously used by the lab to successfully generate flow in microfluidic devices: handheld syringe plunging, handheld pipette pressure generation, and a microfluidic syringe pump. Handheld syringe operation was not feasible for operating the device but was useful for cleaning the device and removing trapped air pockets. Handheld pipettes were suitable

as they are readily available to most labs and offer a reproducible method of generating a negative pressure. A syringe pump was considered for its precision in generating a defined flow rate but is more expensive and less commonly owned than a pipette.

Previous results gathered by the capstone team showed promise with the handheld pipette method for flow generation. As such, this was the planned device operation method for the new device design. Preliminary testing with a low-volume micropipette (2-20 uL) was successful in operating the device using dye to visualize flow in the device under brightfield microscopy. Initial testing with a syringe pump (New Era SyringeONE) was unsuccessful, as flow was nonexistent or too slow to visualize within the device's intended operation period. Future testing will be conducted with a range of syringes and volumes, as well as syringe pump settings to determine if this method is viable for further device evaluation.

Flow cessation was an important characteristic of device operation since it was crucial in allowing CASA measurements on sperm cells. Previous methods have relied on delayed or user-induced pressure release to open both sides of the device (all inlets and the outlet) to atmospheric pressure, which halts flow. Timely flow cessation is also necessary as the sperm cells to be used with this device have a short period of peak motility, which necessitates flow cessation that is as immediate as possible. With a handheld pipette, near-immediate flow cessation can be achieved by simply disconnecting the pipette from the pipette tip. This has currently been observed with dye testing, where a clear shift between convective and diffusive flow regimes was seen, and with microbeads, which come to a stop upon pipette tip disconnection. This method does introduce experimental variability that is currently unaddressed, as the pipette tip / tubing apparatus needs to be restricted as motion causes fluid to rapidly shift in the device. Proposed solutions include removing the tubing completely instead of only the pipette, creating a releasable valve or stopper in part of the tubing or pipette tip assembly, or fixing the tubing/tip such that it will not move after disconnection from the pipette.

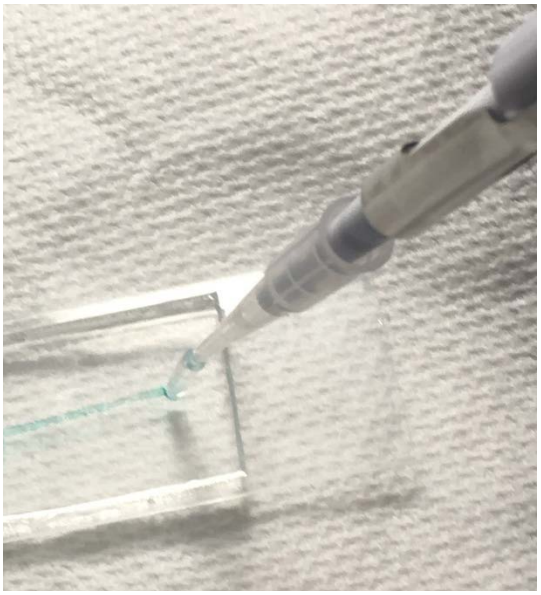

Fig. 11: Microfluidic device shown with tubing connecting the pipette tip to the device outlet. The microdevice is actuated by drawing up a known volume in the pipettor, creating suction to draw samples into the chip for mixing, activation, and analysis.

3.2.2 Mixing evaluation

Multiple methods were used evaluate the device's ability to mix the sample and diluent effectively. Initial testing involved using colored food dye as a visual indicator of mixing, and an image taken from microscope video illustrates this (Fig. 12). Results were similar to those predicted by the COMSOL model (Figs. 13-14), which showed sample streams maintaining their width after introduction to the main channel and mixing occurring when fluid is carried transverse to the direction of flow by the mixing structures. After visually identifying that the mixer was operating as intended, the device was loaded with 6 um polystyrene beads instead of dye, and darkfield video was acquired (Fig. 15).

The intent of observing microbead flow is to analyze bead path lines with PIV software and determine the stability of fluid flow rate over time, as well as to observe and evaluate flow cessation. As of now, these videos are still being processed, and more data needs to be acquired before making a calibration curve linking handheld pipette volume to flow rate generated in the device. Fig. 16 shows an example of darkfield video captured for this purpose, and beads appear as small streaks which flow downstream and interact with the micromixer. Even in the still image, the interaction between the beads and the mixer is visible, as the beads deflect in the direction of the mixing geometry, which pulls fluid towards the channel edge and back towards its center.

Another proposed method for evaluating mixing efficiency was to use a dilute solution containing fluorescein as the sample and use fluorescent microscopy to assess downstream mixing. This method has not yet been used to assess mixing in the device, but work is underway to begin testing trials and compare results to the methods described above.

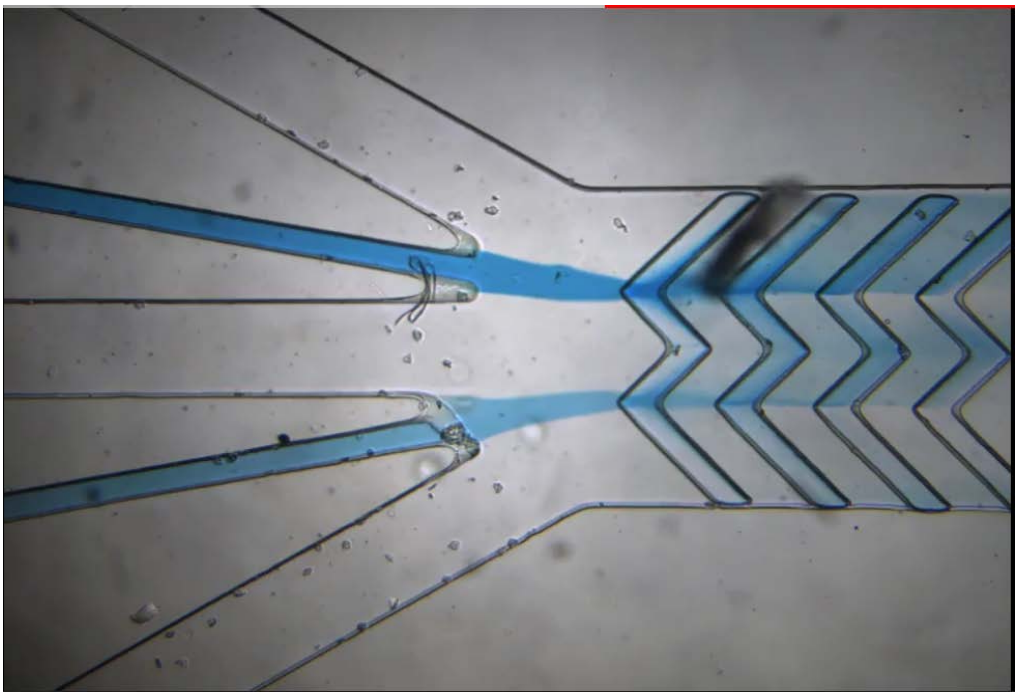

Fig. 12: Brightfield microscopy showing the device during a test operation. Large out-of-focus debris is not inside the channel. The blue streams indicate good alignment of the fluidic layer sperm inlets and the peaks of the chevron mixing structures.

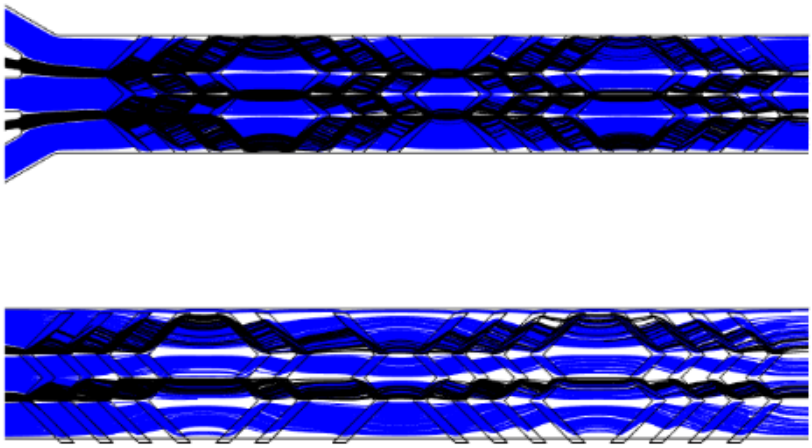

Fig. 13: COMSOL streamline results showing diluent (blue) and sample (black) streams flowing over the mixing region. Top image shows perfectly aligned mixing geometry, while the bottom image shows the same result with a 50 um misalignment of the mixer.

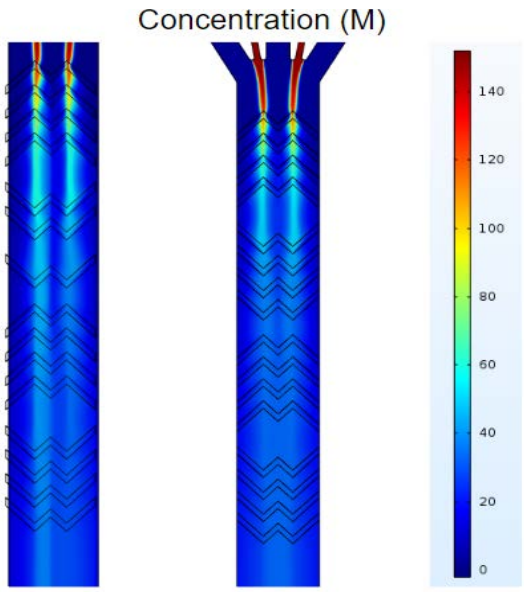

Fig. 14: COMSOL results for dilute species transport shown for an aligned (left) and misaligned (right) mixer.

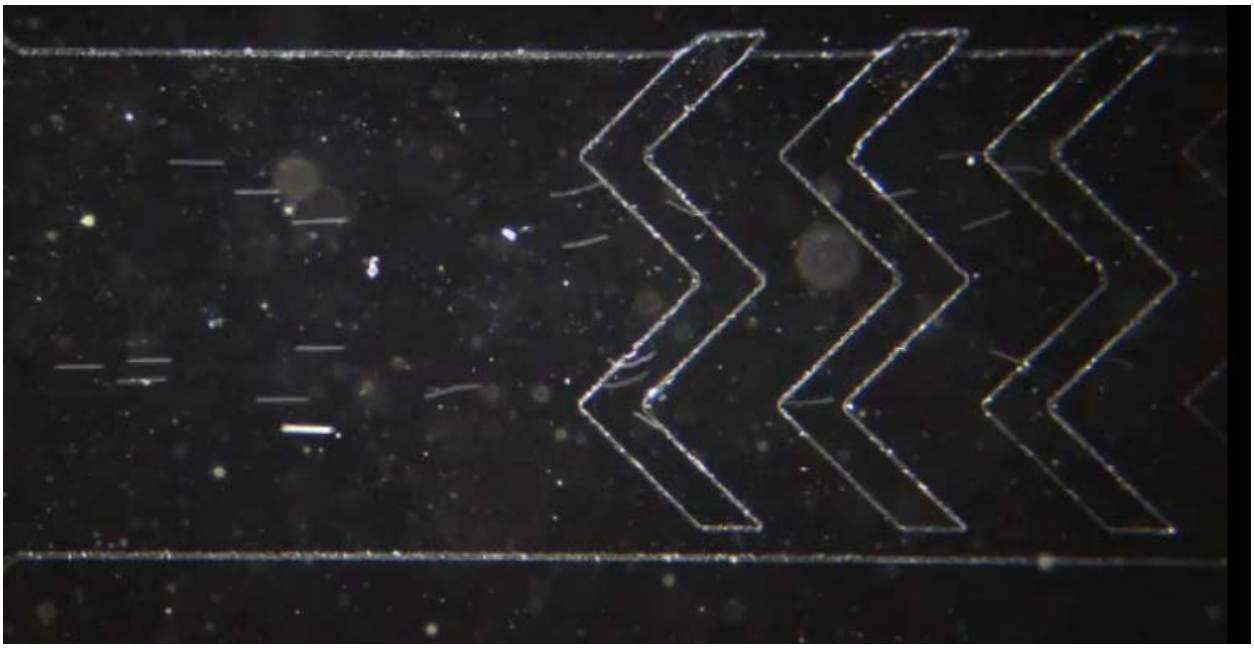

Fig. 15: Darkfield microscopy showing 6um polystyrene beads flowing in an older device with similar mixing structures.

3.2.3 Sperm activation efficiency

Due to the impact of Covid-19, focus of this project was shifted to focus on remote work that could be conducted safely, consisting primarily of computational simulations. Because the difficulty in travelling during the spring spawning season, previously planned collection of sperm from Red Snapper was not executed. The developed device will be used in further studies to evaluate fish sperm sample from laboratory species, such as Zebrafish.

4. Conclusions and Future Recommendations

In this study, a microfluidic device is described which was designed using FEA simulation as a guiding tool, fabricated using multistep photolithography and elastomer curing, and tested with various fluids and samples to evaluate the device's functionality. The goals of this project were to improve the preliminary design created by the capstone engineering team, fabricate the device with soft lithography and evaluate its fluidic operation, and evaluate the device's mixing capabilities and ability to activate fresh- and saltwater fish sperm cells for CASA measurement.

COMSOL Multiphysics and Autodesk Inventor were the main tools used for design and simulation, and two candidate designs were chosen after an iterative design/simulation process. The template mold for the primary design was fabricated using manual mask alignment, which was the most difficult part of the process. This mold was slightly misaligned, but still provided one mold with mixing structures located in the correct region. The device was fabricated by molding a curable elastomer on the template. The device was cut to shape after being peeled from the mold, and access ports were punched to allow sample loading and tubing inserts. Finally, the device was tested for flow initiation/cessation, ease of loading and operation, and preliminary testing was done for evaluating mixing efficiency.

Future work is focused on creating a more reliable method of manual mask alignment, testing the candidate devices against each other with regards to ease of operation and fabrication, and evaluating the device with sperm sample and CASA. A 3D-printed manual mask alignment tool has already been prototyped and fabricated, but not yet used with any microfluidic photomask designs. Work on this device will continue in the near future, and more devices will be fabricated to gain a better understanding of design flaws and difficulties with operation. We envision that this device can serve as a platform for building more complex devices with integrated cell-sensing regions and push forward the movement towards total lab-on-chip assessment of sperm quality, which would benefit aquatic species fisheries.

Acknowledgements

This work was supported by the Louisiana Sea Grant Undergraduate Research Opportunity Program. We thank Jason Eades, Jorge Belgodere, and Jonathan Thomas for contributions with FEA simulation, photomask alignment, and device fabrication, respectively.

References

Alavi, S.M.H., and Cosson, J. (2006) Sperm motility in fishes. (II) Effects of ions and osmolality: a review. Cell biology international 30(1), 1-14

Beckham, J., Alam, F., Omojola, V., Scherr, T., Guitreau, A., Melvin, A., Park, D.S., Choi, J.-W., Tiersch, T.R., and Monroe, W.T. (2018) A microfluidic device for motility and osmolality analysis of zebrafish sperm. Biomedical microdevices 20(3), 67

Benesch-Lee, F., Guevara, J. M., & Albrecht, D. R. (2017, June 5). Multilayer photolithography with manual photomask alignment. Retrieved February 18, 2021, from https://blogs.rsc.org/chipsandtips/2017/06/05/multilayer-photolithography-with-manual-photomask-alignment/?doing_wp_cron=1613608864.4829590320587158203125

Chesney, E.J., Baltz, D.M., and Thomas, R.G. (2000) Louisiana estuarine and coastal fisheries and habitats: perspectives from a fish's eye view. Ecological Applications 10(2), 350-366

Fauvel, C., Suquet, M., and Cosson, J. (2010) Evaluation of fish sperm quality. Journal of Applied Ichthyology 26(5), 636-643

Goodyear, C. (1995) Red snapper in US waters of the Gulf of Mexico. Contrib. MIA-95/96-05. Southeast Fisheries Science Center, Miami Laboratory, Miami ….

Hagedorn, M., Varga, Z., Walter, R.B., and Tiersch, T.R. (2019) Workshop report: Cryopreservation of aquatic biomedical models. Cryobiology 86, 120-129

Kashaninejad, N., Shiddiky, M.J.A., and Nguyen, N.T. (2018) Advances in Microfluidics-Based Assisted Reproductive Technology: From Sperm Sorter to Reproductive System-on-a-Chip. Advanced Biosystems 2(3), 1700197

Kirby, B. J. (2013). 4.5 Laminar flow patterning in microdevices. In Micro- and nanoscale fluid mechanics: Transport in microfluidic devices. Cambridge: Cambridge University Press.

Liu, Y., Blackburn, H., Taylor, S.S., and Tiersch, T.R. (2019) Development of germplasm repositories to assist conservation of endangered fishes: Examples from small-bodied livebearing fishes. Theriogenology 135, 138-151

Riley, K.L., Holladay, C.G., Chesney, E.J., and Tiersch, T.R. (2004) Cryopreservation of sperm of red snapper (Lutjanus campechanus). Aquaculture 238(1-4), 183-194

Whitesides, G.M. (2006) The origins and the future of microfluidics. Nature 442(7101), 368

Williams, K., Papanikos, N., Phelps, R.P., and Shardo, J.D. (2004) Development, growth, and yolk utilization of hatchery-reared red snapper Lutjanus campechanus larvae. Marine Ecology Progress Series 275, 231-239